Technical Report

UDC 629 . 11 . 012 . 1 : 539 . 43

Fatigue Property of Railway Axles for Shinkansen Vehicles

Taizo MAKINO* Hiroki SAKAI

Abstract

Railway axles are ranked as the most important security parts because their fractures directly cause derailment of vehicles. However, press-fitted seats with wheels are necessary in axles due to the needs for structural function. Damages due to fretting fatigue occasionally occur on the seats in axles. Thus induction hardening and improvement of shape of press-fitted part have been adopted in axles for Shinkansen vehicles. In the present paper, a prediction method for fretting fatigue strength using fracture mechanics approach is constructed and validated. Moreover, full-scale induction hardened axles are fatigue-tested under 1.5 times higher stress than the allowable stress for design. Neither fracture nor magnetic particle flaws are indicated after the test.

1. Introduction

Among the many parts that make up a railway vehicle, axles are considered the most important safety-related items because a broken axle can directly lead to derailment. The fatigue damage of axles has long been studied since A. Wöhler[1] worked out the Wöhler diagram (S-N diagram) in the 19th century. Securing sufficient strength reliability of axles is still an important challenge for mechanical engineers.

Because of their construction, axles are provided with press-fitted seats with wheels; these seats are subject to fretting fatigue under certain circumstances. Therefore, studies on axle fatigue have focused on the phenomenon of axle fatigue due to the fretting of press-fitted seats.

This technical report first outlines the axles for railway vehicles and describes the salient characteristics of fretting damage—a phenomenon that often occurs with axles. Then, concerning the fatigue properties of axles, especially the fretting fatigue property, the report explains the prediction of axle fatigue strength made by one researcher by applying fracture mechanics. Finally, it presents the results of our recent fatigue test using full-scale axles.

2. Outline of Axles

At Nippon Steel & Sumitomo Metal Corporation, axles for railway vehicles began to be manufactured as steel castings around 1901 when the former Sumitomo Casting Works was established. They were eventually replaced by steel forgings in 1917. According to the company's history, the materials used for these axles were purchased from the former government-managed Yawata Steel—the predecessor of the company. Since around 1955, they have been supplied by Wakayama Works. In the meantime, the efficiency of axle production improved dramatically thanks to the introduction of a high-speed precision forging machine, special heat-treatment line, etc. In the early 1960s, sometime before the opening of the Shinkansen, the company developed induction-hardened axles having a larger load bearing capacity than conventional ones through a joint research project with the Japanese National Railways. These axles were first employed in electric locomotives and were later adopted in large quantities for the Shinkansen, established in 1964. However, the influences of shapes of press-fitted parts and induction hardening conditions on the fatigue strength of axles were not completely known. In fact, the induction hardening conditions and shapes of press-fitted parts have been continually improved through energetic research activities.

For the axles used in Japan, JIS E 4502 [2,3] and JRIS J 0401 [4] specify the axle classes, material chemical compositions and mechanical properties, manufacturing processes, representative shapes, etc. The axle specifications in JIS E 4502 are described in a separate article[5] of this issue. In this technical report, we focus on the induction-hardened axles for high-speed railway vehicles specified in JRIS J 0401. The mechanical properties and heat treatment process specified for induction-hardened axles are shown in **Table 1**. As shown, the material is JIS S38C steel, and the mechanical properties are obtained after quenching and tempering (before induction hardening).

Figure 1 shows induction hardening region in an axle.[4] It can be seen that the entire axle surface is induction hardened, except for the

* Chief Researcher, Dr.Eng., Materials Reliability Research Lab., Steel Research Laboratories
1-8 Fuso-cho, Amagasaki, Hyogo 660-0891

Table 1 Mechanical properties and heat treatment of induction hardened axles for high speed vehicle [4)]

Class	Material	Application	Mechanical properties before induction hardening				Heat treatment
			Yield strength	Ultimate tensile strength	Elongation	Reduction of area	
Induction hardened axle	JIS S38C	Powered and non-powered axles for high speed vehicle	≥ 294 MPa	≥ 539 MPa	≥ 25 %	≥ 45 %	Firstly quenching & tempering, secondly induction hardening and tempering

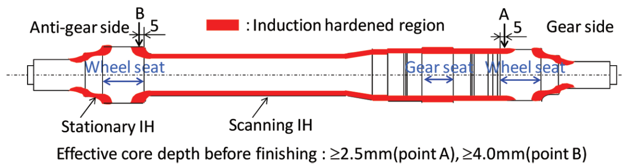

Fig. 1 Induction hardening region in an axle [4)]

central part of each wheel seat to which a wheel is press fitted. For points A and B in the figure, JRIS J 0401 specifies that the effective core depth (i.e., the region exceeding HV400) before finishing should not be less than 2.5 and 4.0 mm, respectively.[4)] The reason why the central part of each wheel seat is not induction hardened is that a different method of induction hardening is applied to the gear side of wheel seat (stationary IH) and the counter-gear side of wheel set (scanning IH). Since a wheel is press fitted to each wheel seat, the stresses that occur in this part are sufficiently small to pose any problem of strength.

Figure 2 shows the distributions of Vickers hardness and axial residual stress in the hardened layer in the neighborhood of a wheel seat after induction hardening.[6,7)] As shown in Fig. 2 (a), the surface hardness is in the range HV500 to HV550, and the effective core depth is 4-5 mm. The hardness distribution was measured at a point corresponding to point B in Fig. 1, and hence, the above specification (4.0 mm or more at point B) is met. According to Fig. 2 (B), the residual stress at the surface is a compressive stress of about −600 MPa, and the depth at which the residual stress changes from compressive to tensile is 10-20 mm.

3. Fretting Damage to Press-Fitted Seats of Axle

3.1 Characteristic of fretting damage

Each axle is used with a wheel press fitted to each of the two wheel seats, the larger-diameter portions near both ends of the axle, as shown in Fig. 1. (The axle press fitted with wheels is called a wheel set.) Unless otherwise specified by the client, the interference for wheel press-fitting (i.e., difference between wheel seat diameter and hub bore diameter) is so controlled that the press-fitting ratio (i.e., ratio of press-fitting interference to axle diameter) becomes 1.4/1,000 for standard and 1.5/1,000 for maximum.[8)] As a result, the nominal contact pressure between the axle and wheel is 50-70 MPa.

Figure 3 shows the external forces that act upon a wheel set.[9)] As shown, a vertical force is applied near each end of the axle via a bearing, while a reaction force (also in vertical direction) is applied to the surface of contact between the axle and rail. In addition, in a curved railway section, a lateral force produced by the contact between the wheel and rail is applied toward the outer rail. At this moment, the wheel set is put under the typical rotational bending stress.

On the other hand, fretting refers to repeated occurrence of a microslip between contact surfaces. When fretting continues for a long period of time, a brown powder called cocoa gradually accumulates

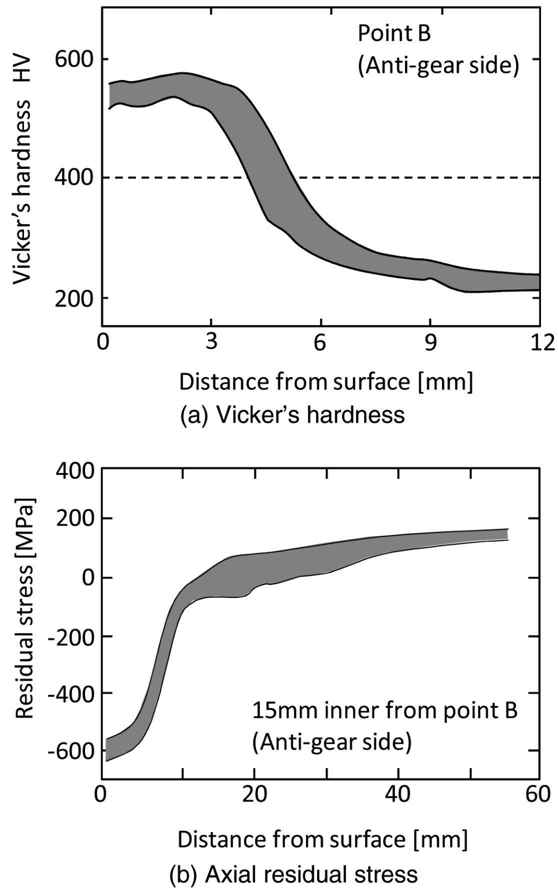

Fig. 2 Distributions of Vicker's hardness and axial residual stress at wheel seat after induction hardening [6,7)]

at the contact surfaces, from which the powder is then partly discharged. This phenomenon is called fretting corrosion. Since fretting causes the wear to progress and the fatigue strength to decline, the damage induced by fretting is called fretting damage.

Under no load, the axle and press-fitted wheels look like a completely solid thing. However, when they are put under a rotational bending load as shown in Fig. 3, the wheel deformation fails to completely follow up the axle bending deformation, and as a result, a micro relative slip induced by the difference in deformation occurs near the end of the press-fitted part as shown in **Fig. 4**. Therefore, the press-fitted parts are highly susceptible to fretting. **Figure 5** shows the fretting corrosion region of a press-fitted part of axle observed under an optical microscope. The microphotographs were taken after the fretting corrosion was removed by buffing from an actual-size axle subjected to a fatigue test. They reveal microscopic surface irregularities, pits, stuck wear debris, and fine fatigue cracks.

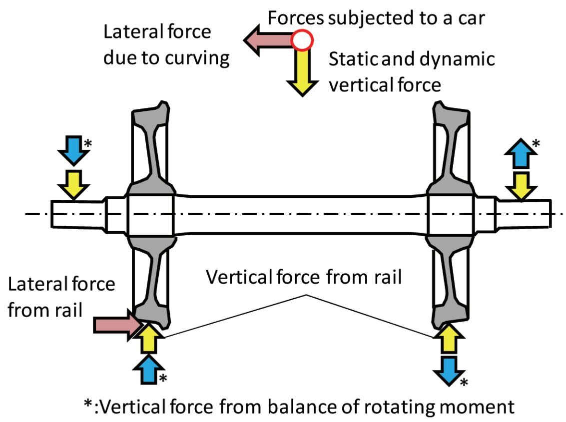

Fig. 3 Forces subjected to a wheel-axle assembly

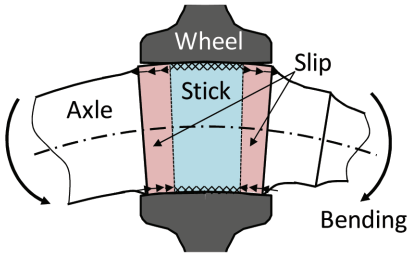

Fig. 4 Schematic illustration of bending deformation at press-fitted part of an axle

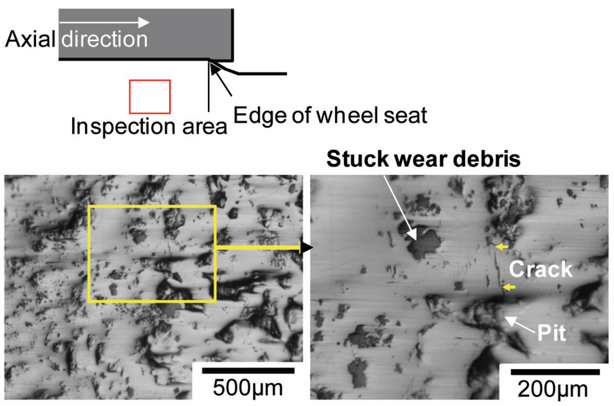

Fig. 5 Photos of optical microscope of fretting corrosion region inspected on press-fitted surface of axle

3.2 Influence of induction hardening

In the preceding section, we explained that the axles for Shinkansen vehicles that are put under large loads during operation are subjected to induction hardening as a measure to prevent fretting damage to them. From the standpoint of preventing fretting damage, induction hardening is very effective, since it increases the hardness of the axle and produces a large compressive residual stress in it. In particular, the compressive residual stress helps restrain the propagation of fretting fatigue cracks by keeping them from opening.

Figure 6 shows the relationship between surface residual stress and fretting fatigue limit.[10] The figure plots both fatigue limit σ_{w1} for crack initiation and fatigue limit σ_{w2} for crack propagation or fracture obtained with several small-diameter to full-scale axles. It can

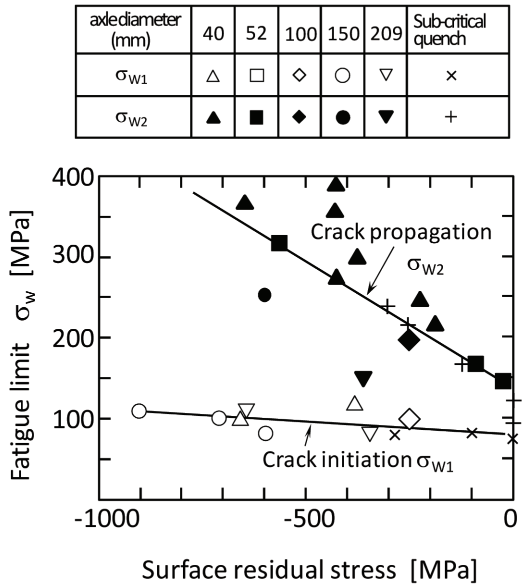

Fig. 6 Relationship between surface residual stress and fretting fatigue limit [10]

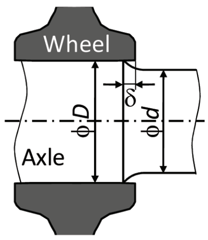

Fig. 7 Definition of diameter ratio and overhang distance

be seen that the larger the compressive residual stress, the higher the value of σ_{w2}, although it depends more or less on the axle diameter and residual stress distribution. On the other hand, σ_{w1} is lower than σ_{w2} and almost unaffected by the residual stress. The fact that σ_{w2} is considerably higher than σ_{w1} suggests that the compressive residual stress is really effective in restraining the propagation of fretting fatigue cracks.

3.3 Influence of shape of press-fitted parts

The shape of the axle portion near the end of each press-fitted part significantly influences the axle fretting fatigue. As the main parameters of the shape of that portion, diameter ratio D/d and overhang distance δ are shown in **Fig. 7**. The diameter ratio is the ratio of diameter D of the press-fitted portion to the diameter d of the non-press-fitted portion, and overhang refers to the state of the wheel seat edge shifting inward from the wheel edge. Also, δ is defined as the distance covered by the said shift.

Figure 8 shows the influences of diameter ratio D/d and overhang distance δ on the fatigue strength of small-diameter press-fitted axles.[11-13] In addition to σ_{w2}, the figure shows $\sigma_{w1,\,mag}$ for the occurrence of flaws detected by magnetic particle inspection and $\delta_{w1,\,mic}$ for the initiation of fine cracks confirmed under an optical microscope. They form nearly the same curve. It can be seen from the figure that high fatigue strength can be secured by equating D/d to 1.1 or more and by equating δ to a positive value. These influences of the shape of press-fitted parts are considered owing to the changes

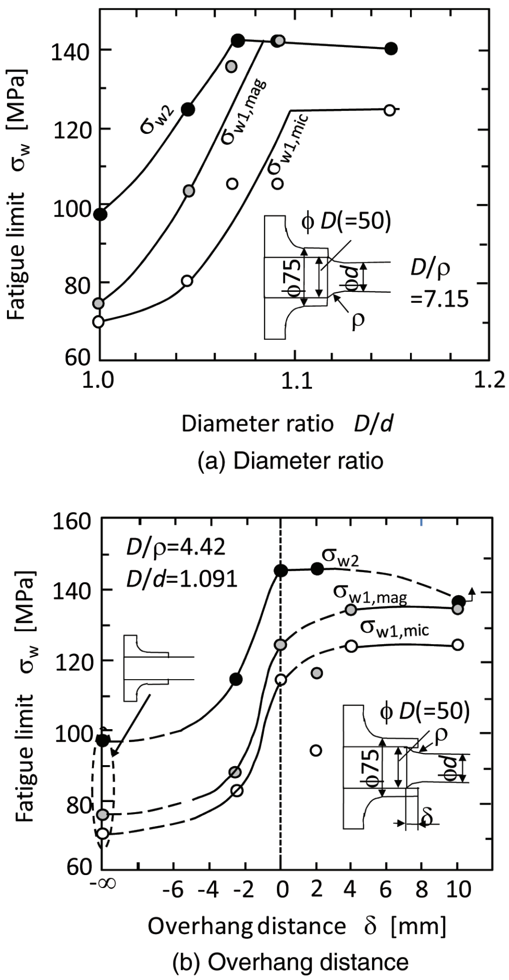

Fig. 8 Effect of diameter ratio and overhang distance on fatigue limit of small-scale press-fitted axles [10-12]

in stress concentration, contact surface pressure distribution, and relative slip. Although the contribution of each of these factors is not completely clear, we consider that the improvement in fatigue strength is attributable largely to a decrease in stress concentration and relative slip. It is difficult to make the *D*/*d* of Shinkansen vehicles sufficiently large because they are subjected to induction hardening, as mentioned earlier. To compensate for this effect, an overhang is given to them.

4. Prediction of Fatigue Strength Applying Fracture Mechanics[14]

As described so far, the fretting fatigue strength of the press-fitted parts of axles depends on whether the fretting fatigue cracks propagate. Since the propagation limit of a fatigue crack can be predicted by a technique that employs the principles of fracture mechanics, it should be possible to apply a similar technique to predict the fretting fatigue strength of press-fitted parts of axles. Therefore, we apply fracture mechanics to evaluate the propagation characteristics of fretting fatigue cracks in small-diameter press-fitted axles and establish a method of predicting the fretting fatigue strength of press-fitted axles.

4.1 Fatigue characteristics of small-diameter press-fitted axles

To obtain the basic data required to establish a prediction method

Table 2 Classification of tested press-fitted axle and fatigue limit

Class.	Axle diameter (mm)	Case depth (mm)	Surface hardness HV	Peak of compressive residual stress	Faigue limit σ_{w2}
QT	40	-	200	-	110 MPa
IH04	38	0.4	520	−600 MPa	270 MPa
IH20	40	2.0	600	−820 MPa	>320 MPa

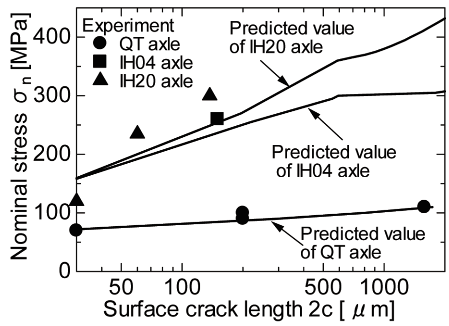

Fig. 9 Relationships between surface crack length inspected on run-out axle and test stress amplitude and their comparison with predicted values [14]

mentioned above, we conducted a fretting fatigue test using press-fitted axles that are 38-40 mm in diameter. Each of the test pieces was composed of a shaft and a boss, which was press fitted to the center of the shaft with an interference that would produce nearly the same surface pressure as that in an actual axle. The materials used were JIS S38C steel for the shafts and wheel steel for the bosses. As shown in **Table 2**, three types of test pieces were used—the QT axle that was quenched and tempered, the IH04 axle that was induction-hardened to a comparatively small depth, and the IH20 axle that was induction hardened to a comparatively large depth.

The three types of test pieces mentioned above were subjected to a three-point rotational bending fatigue test. As a result, the fatigue limits for fracture (σ_{w2}) shown in the rightmost column of Table 2 were obtained. Then, with each of the test pieces that withstood stresses under σ_{w2} up to 2×10^7 cycles, the condition of occurrence of fretting fatigue cracks in the surface of the press-fitted part was observed. **Figure 9** shows the relationship between confirmed surface crack length and test stress. We can draw the following conclusions from the figure: 1) the crack length increases with the rise in test stress, 2) the stress required for crack propagation to a certain length for the IH04 and IH20 axles is higher than that for the QT axle, and 3) induction hardening increases the resistance to propagation of microcracks.

4.2 Stress state in press-fitted axles and evaluation thereof applying fracture mechanics

In this subsection, we analyze the stress state in press-fitted axles using the finite element method (FEM). The finite element mesh used in the analysis is shown in **Fig. 10**. As schematically shown in the figure, the boss model is partly rounded at the press-fitted end. The reason is as follows. In a separate study,[15] it was found that the part that experienced a stress concentration coincided with the part that experienced a crack, during the FEM analysis of a model that faithfully reproduced the surface profile of the part near the press-fitted end. **Figure 11** shows the axial stress distribution obtained

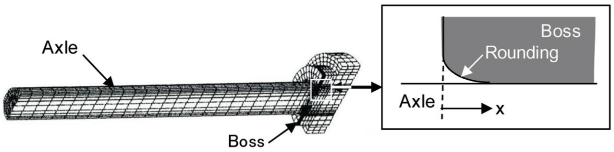

Fig. 10 FE analysis model for press-fitted axle [14]

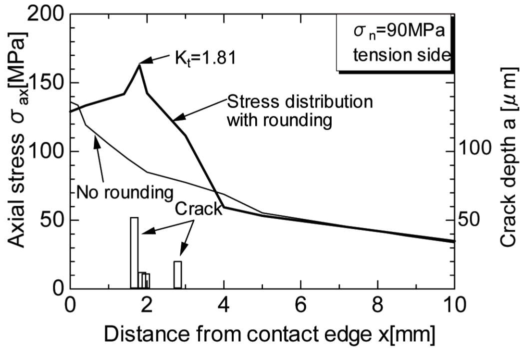

Fig. 11 Comparison between axial stress distribution obtained from FE analysis and crack initiation points inspected after fatigue test [15]

from the FEM analysis in comparison with the crack initiation points observed in the fatigue test. As shown in the figure, the maximum stress increases as the point of occurrence of maximum stress shifts from the press-fitted end inward owing to the effect of rounding, and the point of maximum stress corresponds to the crack initiation point observed in the fatigue test.

The basic concept of the fracture-mechanics-based evaluation in the present study is that a crack is assumed to exist in the part being evaluated and the possibility of propagation of that crack is judged by using the stress intensity factor, which is one of the parameters of fracture mechanics. First, on the assumption that there were cracks of varying depth in the press-fitted part, their stress intensity factors were obtained by using the above FEM analysis results and conventional formula[16] and the range of variation during the fatigue test was taken as ΔK. The range of stress intensity factor that represents the non-propagating limit of crack is called the threshold stress intensity factor range ΔK_{th}, which is based on the assumption that the cracks of dimensions plotted in Fig. 9 remain non-propagating. The relationship shown in **Fig. 12** was obtained from the stress intensity factor range. Surface crack length was converted to depth a in Fig. 9 on the basis of the crack aspect ratio confirmed experimentally. It can be seen from Fig. 12 that ΔK_{th} of microcracks depends on crack size and residual stress. Taking this characteristic of ΔK_{th} into consideration, the values of ΔK_{th} plotted in Fig. 12 were approximated by the following equation.

When $a < a_{cr}$,

$$\Delta K_{th} = \Delta K_{th\infty}\,(a/a_{cr})\,\alpha \qquad (1)$$

Here $\Delta K_{th\infty}$ denotes the threshold stress intensity factor range for long cracks (value obtained by a crack propagation test carried out separately, at stress ratio 0, it is 5 MPa$\sqrt{m}$ for QT axle and 3 MPa$\sqrt{m}$ for IH04/20 axles); a_{cr} is the critical crack length (0.26 mm for QT axle and 0.09 mm for IH04/20 axles), and α is a constant (0.55; inclination against a of ΔK_{th}, obtained by least square approximation of QT axle data). Concerning the residual stress dependency of $\Delta K_{th\infty}$, we derived an approximate equation showing that the value of $\Delta K_{th\infty}$ increases with the increase in compressive residual stress. However, it has been omitted owing to space constrains.

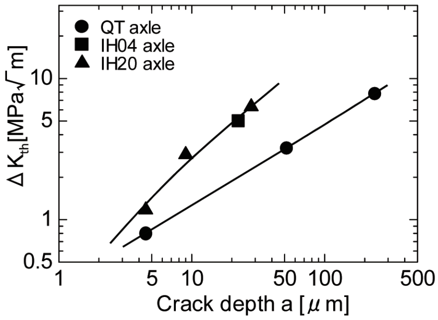

Fig. 12 elationship between ΔK_{th} and crack depth [14]

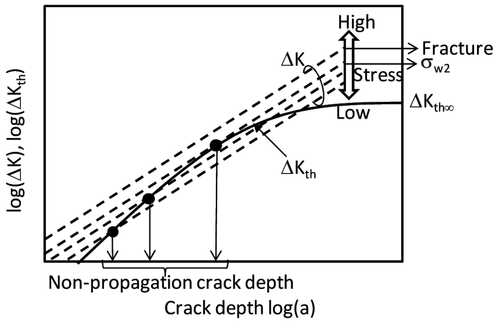

Fig. 13 Schematic illustration indicating how to predict non-propagation crack size and fatigue limit

Table 3 Comparison between experimental and predicted σ_{w2} [14]

Class.	Experimental σ_{w2} (MPa)	Predicted σ_{w2} (MPa)
QT	110	110
IH04	270	310
IH20	>320	540

As schematically shown in **Fig. 13**, the values of ΔK and ΔK_{th} obtained above were compared with each other to predict the propagation and non-propagation behaviors of cracks. Namely, it is predicted that the crack propagates when ΔK is larger than ΔK_{th}, as well as when they are equal to each other (i.e., at the point of intersection in Fig. 13). In Fig. 9, the predicted sizes of non-propagating cracks are shown by solid lines. It can be seen that they agree well with the plotted experimental values. In Fig. 13, when the stress increases to a certain point, ΔK and ΔK_{th} no longer intersect. This critical stress is expected to be the fracture fatigue limit σ_{w2}. **Table 3** shows the experimental and predicted values of σ_{w2} for the three types of test pieces. They agree fairly well, suggesting that our fatigue strength prediction method described above is valid.

5. Fatigue Characteristics of Full-scale Axles

The fatigue characteristics of full-scale induction-hardened axles of the current specifications have been evaluated by Motomatsu et al.,[17] Ishizuka et al.,[18] and Isomura.[19] It has been found that the fatigue limit $\sigma_{w1,\,mic}$ of those axles is 70 MPa. On the other hand, as for $\sigma_{w1,\,mag}$ and σ_{w2}, a study has established that neither fractures nor magnetic particle flaws occurred during a fatigue test of up to 2 × 10^7 cycles under 177 MPa. The permissible design stress for induction-hardened axles is specified to be 147 MPa in JIS E 4501[9]—the standard for strength design methods for axles. Therefore $\sigma_{w1, mag}$ and σ_{w2} for the above axles are about 1.2 times the permissible stress. However, the true margin against fatigue fracture has not yet been clarified because of limitations on the loading capacity of conventional fatigue testers.

Under this condition, a fatigue test was conducted with full-scale induction-hardened axles by using a newly introduced fatigue tester[20] exclusive for full-scale railway wheels and axles.

5.1 Axle tested and fatigue test method

The tested axle was induction hardened and intended for simulating an axle for Shinkansen T vehicle. The shape of the axle is shown in **Fig. 14**. The wheel seat diameter is 166 mm and the diameter ratio (D/d) is 1.038. The test piece faithfully reproduces the actual axle shape from the wheel seat to the axle body. The wheel seat on one side of the test piece is press fitted with a member corresponding to a wheel in such a way that the overhang becomes equal to that of the actual axle.

Figure 15 shows the structure of the fatigue tester used.[20] On the tester, the test piece is set in vertical position with the wheel member facing down. The test piece is repeatedly subjected to a bending load by a resonance produced by rotating eccentric masses at the axle end opposite to the end fitted with the wheel member.

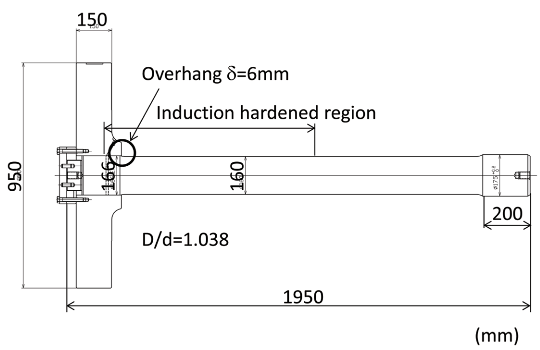

Fig. 14 Configuration of a tested full-scale axle assembly

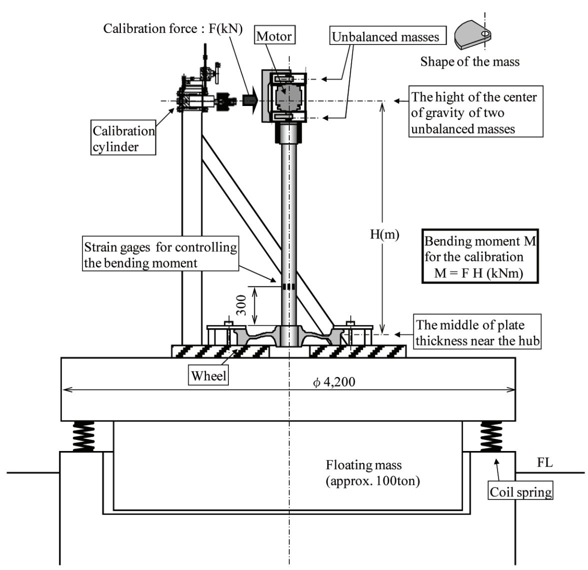

Fig. 15 Structure of fatigue testing machine for full-scale wheel and axle assembly[20]

5.2 Fatigue test results

The fatigue test was conducted by using two different stress levels, with the nominal wheel seat stresses being 150 and 220 MPa—the maximum capacity of the tester. Under both conditions, the test piece did not fracture in the test that was completed after the load was applied 2×10^7 cycles. **Figure 16** shows the test results on an S-N diagram for comparison with test results obtained in the past.[17,19] It can be seen from the figure that the higher test stress used in the present test is still higher than the maximum stress ever tested in the past. After the fatigue test, the wheel member was pulled out from the axle, and the wheel seat surface was subjected to a magnetic particle inspection. As a result, the test pieces revealed no magnetic particle flaws. Therefore, the values of $\sigma_{w1, mag}$ and σ_{w2} for the induction-hardened axle were 220 MPa or more, i.e., 1.5 times or more that of the permissible design stress.

In Europe, for high-speed railway vehicles, low-alloy steel axles called EA4T, specified in the European Standards EN13261,[21] are most commonly used. Concerning the fatigue strength of press-fitted parts of EA4T, the evaluation data of Murawa have been published. According to the data, σ_{w2} is 110 MPa or more when $D/d = 1.03$ and 145 MPa or more when $D/d = 1.08$.[22] Therefore, with a given D/d ratio, the fatigue strength of the induction-hardened axle is more than twice that of the EA4T axle.

Figure 17 shows an optical microphotograph of a fretting corrosion region on the surface of a wheel seat of axle observed after a fatigue test under 220 MPa. The photo reveals cracks up to 0.53 mm in length. The implication is that the fatigue test ended at the time when the above crack length was reached. Considering that the number of test cycles had reached 2×10^7, it is estimated that the cracks had stopped propagating. Therefore, it should be possible to

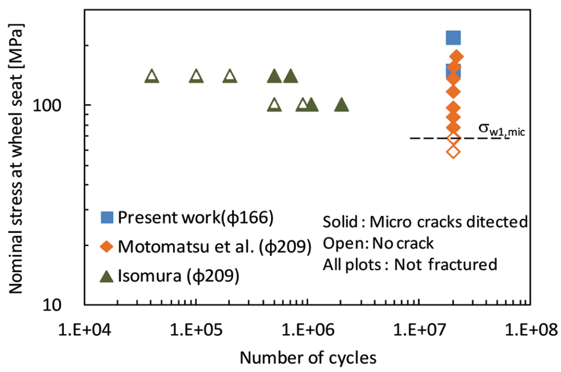

Fig. 16 S-N diagram for full-scale axles

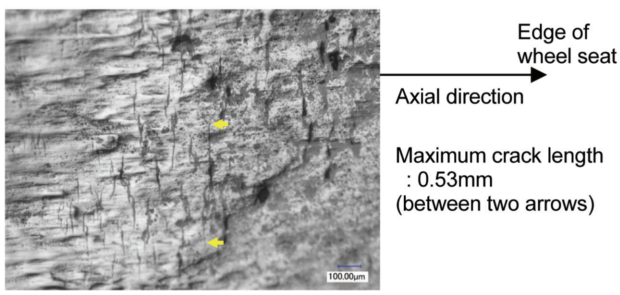

Fig. 17 Photo of optical microscope of fretting corrosion region inspected on wheel seat of axle after fatigue test (σ = 220 MPa, N = 2×10^7)

apply the fatigue strength prediction method based on fracture mechanics discussed in the preceding section to full-scale induction-hardened axles as well. We plan to intensively study the prediction method in future.

6. Conclusion

In this technical report, we outlined the axles for railway vehicles and described the characteristics of fretting damage—a phenomenon unique to these axles. To secure the desired fretting fatigue strength of axles, it is effective to introduce an appropriate compressive residual stress to them by induction hardening and provide the axle press-fitted parts with a suitable overhang. As part of the results of continued R&D, those methods are employed for axles of Shinkansen vehicles. Since the fretting fatigue strength of axles is governed by the propagation behavior of fatigue cracks, it can be predicted by applying fracture mechanics. Therefore, we developed a method for predicting the fretting fatigue strength of small-diameter induction-hardened axles and verified the usefulness of the method.

Concerning full-scale induction-hardened axles, a newly introduced fatigue tester was employed to test their fatigue strength under conditions more rigorous than those used in previous fatigue tests. As a result, although neither magnetic particle flaws nor fractures could be generated, we could clarify that the fatigue limit to fretting damage was 220 MPa or more, i.e., 1.5 times or more of the permissible design stress. This means that the induction-hardened axles are much higher in fatigue strength than the European EA4T axles with proven performance.

An induction-hardened axle having a large difference in diameter between the wheel seat and the axle body may be cited as a futuristic axle. If such an axle could be developed, it would become possible to significantly reduce the diameter of the axle body (at present, this can hardly be done because of the limitations set by the induction hardening process), which in turn would make it possible to reduce the axle weight appreciably. In addition, as mentioned earlier, increasing the difference in diameter (i.e., diameter ratio) should help improve the fatigue strength of press-fitted parts. At present, however, in addition to the above limitations set by the induction hardening process, there are several problems to solve, such as the limited capacity of fatigue testers and the absence of the permissible design stress variables for each diameter ratios (i.e., we use a fixed permissible design stress regardless of the diameter ratios). We consider it necessary to tackle those problems in earnest.

As pointed out in a separate article[5] in this issue and by Hirakawa et al.,[23] another step toward the future is to conduct an in-depth study of the way the railway operators use, inspect, and maintain the axles and thereby develop rational new methods of axle design and inspection and decide optimum periods of axle inspections. To this end, it is indispensable to accumulate relevant data through the measurement of stresses occurring in the axles during revenue operation of trains[24] and the simulation of railway vehicle dynamics[25] and develop techniques to estimate the actual load spectrum, predict the axle life, and judge the safety against fatigue damage.

In either case, the above challenge calls for long, strenuous efforts of not only the design, manufacturing, and R&D departments of Nippon Steel & Sumitomo Metal but also the railway operators, universities, and public research institutes. In this respect, we think we should take this initiative.

References

1) The Society of Materials Science, Japan, Committee on Fatigue of Materials: History of Study on Metal Fatigue. 1988, p. 31
2) Japanese Industrial Standards JIS E 4502-1-2001 Axles for Railway Rolling Stock – Quality Requirements
3) Japanese Industrial Standards JIS E 4502-2-2001 Axles for Rolling Stock – Dimensional Requirements
4) Japan Association of Rolling Stock Industries Standards JRIS J 0401-2007 Rolling Stock – Induction-Hardened Axles for High Speed Vehicle
5) Yamamoto, M.: Shinnittetsu Sumikin Giho. (395), 34 (2013)
6) Makino, T., Kato, T., Hirakawa, K.: Engineering Fracture Mechanics. 78 (5), 810 (2011)
7) Committee for Studies on Wheelsets for High Speed Railway Vehicles: Tetsudo Rinjiku (Railway Wheelsets). 1st Edition. Tokyo, Maruzen Planet Corporation, 2008, p. 110
8) Japanese Industrial Standards JIS E 4504-1-2000 Wheelsets for Railway Rolling Stock – Quality Requirements
9) Japanese Industrial Standards JIS E 4501-1995 Railway Rolling Stock – Design Methods for Strength of Axles
10) Hirakawa, K., Toyama, K.: Fretting Fatigue ESIS18. Mechanical Engineering Publications. Waterhouse, R.B., Lindley, T.C. Eds., London, John Wiley & Sons, 1994, p. 461
11) Toyama, K., Inoue, J.: Sumitomo Metal. 48 (2), 13 (1996)
12) Nishioka, K., Komatsu, H.: Transactions of the Japan Society of Mechanical Engineers. 38 (305), 27 (1972)
13) Nishioka, K., Komatsu, H.: Transactions of the Japan Society of Mechanical Engineers. 33 (248), 503 (1967)
14) Makino, T., Yamamoto, M., Hirakawa, K.: ASTM STP 1367 Fretting Fatigue: Current Technology and Practices. Hoepner, D. W., Chandrasekaran, V., Elliot, C. B., Eds., Baltimore MD, ASTM, 2000, p. 509
15) Makino, T., Yamamoto, M., Hirakawa, K.: Transactions of the Japan Society of Mechanical Engineers Series A. 63 (615), 2312 (1997)
16) Kopsov, I. E.: Int. J. Fatigue. 14(6), 399 (1992)
17) Motomatsu, K., Tezuka, K., Maebashi, E.: Railway Technical Research Institute Report. 6 (3), 29 (1992)
18) Ishizuka, H., Akama, M., Hanaoka, T., Satoh, Y., Motomatsu, K., Tezuka, K.: Transactions of the Japan Society of Mechanical Engineers Series A. 60 (578), 2200 (1994)
19) Isomura, S., Yomoda, K.: 11th International Wheelset Congress. Paris, 1995, Vol. 2, p. 51
20) Okagata, Y., Kiriyama, K., Kato, T.: Fatigue Fract. Engng. Mater. Struct. 30, 356 (2007)
21) BSEN13261-2009, "Railway Applications—Wheelsets and Bogies—Axles Product Requirements"
22) Murawa, F.: 15th International Wheelset Congress. Prague, 2007
23) Hirakawa, K.: Derailment Accident of German ICE-3 Intercity Express in Köln – Why the Metal Fatigue of Railway Axles Happened. 1st Edition. Tokyo, Keibunsha, 2009, p. 122
24) Sakai, H., Yamamura, Y., Ogino, T., Iwamoto, A., Togami, Y., Hashimoto, M.: Proceedings of the 18th Jointed Railway Technology Symposium (J-RAIL). 2011, J16426
25) Yamazaki, Y., Yamamoto, M., Kondo, O., Yamamura, Y., Sakai, H., Tanabe, H., Hashimoto, I.: Proceedings of the 19th Jointed Railway Technology Symposium (J-RAIL). 2012, p. 3211

Taizo MAKINO
Chief Researcher, Dr.Eng.
Materials Reliability Research Lab.
Steel Research Laboratories
1-8 Fuso-cho, Amagasaki, Hyogo 660-0891

Hiroki SAKAI
Railway Wheel & Axle Div.
Osaka Steel Works
Railway, Automotive & Machinery Parts Unit